We are IntechOpen, the world's leading publisher of Open Access books
Built by scientists, for scientists

6,900
Open access books available

185,000
International authors and editors

200M
Downloads

154
Countries delivered to

Our authors are among the

TOP 1%
most cited scientists

12.2%
Contributors from top 500 universities

CLARIVATE ANALYTICS
BOOK CITATION INDEX
INDEXED

WEB OF SCIENCE™

Selection of our books indexed in the Book Citation Index
in Web of Science™ Core Collection (BKCI)

Interested in publishing with us?
Contact book.department@intechopen.com

Numbers displayed above are based on latest data collected.
For more information visit www.intechopen.com

Balancing the Spatial and Spectral Quality of Satellite Fused Images through a Search Algorithm

Consuelo Gonzalo-Martín[1] and Mario Lillo-Saavedra[2]
[1]*Dep. de Arquitectura y Tecnología de Sistemas Informáticos, Facultad de Informática,*
Universidad Politécnica de Madrid, Campus de Montegancedo, Boadilla del Monte, 28660
[2]*Dep. de Mecanización y Energía, Facultad de Ingeniería Agrícola,*
Universidad de Concepción
[1]*Spain*
[2]*Chile*

1. Introduction

Image fusion can be understood as the synergetic combination of information provided from several sensors or by the same sensor in different scenarios. The decrease of redundant information, while emphasizing relevant information, not only improves image-processing performance but it also facilitates their analysis and interpretation.

In the last decade, the most used image fusion strategies were based on multi-resolution analysis techniques. Their objective was to find a discrete transform that minimizes the intrinsic uncertainty associated to the joint representation of information. From this point of view, the Discrete Wavelet Transform (DWT) can be considered as the most popular approximation Garguet-Duport et al. (1996).

The DWT is a linear transformation that is very useful in the signal processing area, where one of its principal applications consists in separating data sets into distinct frequency components, which are then represented on common scales. There are different ways of calculating the DWT, among which the most important is the pyramidal algorithm of Mallat Mallat (1989).The fusion method based on Mallat algorithm Pohl & J.L.Genderen (1998); Ranchin & Wald (2000); Zhou et al. (1998) has been one of the most widely used, since it provides fused images with a high spectral quality; however, its low anisotropic nature still produces some problems for the fusion of images with a high content of borders that are not horizontal, vertical or diagonal Candès & Donoho (2000). Dutilleux (1989) has proposed a Wavelet *à trous* (with holes) algorithm. This algorithm differs from the pyramidal ones in that it presents an isotropic nature and is redundant, which implies that between two consecutive degradation levels, there is no dyadic spatial compression of the original image; but rather the size of the image is maintained. Several works, have showed that redundant DWT provides better results in determined image processing applications such as noise elimination Malfait & Roose (1997), texture classification Unser (1995); Zou & Jiang (2010), and in the case of image fusion Chibani & Houacine (2003); Nunez et al. (1999); Yang et al. (2010).

Despite the good results provided by the DWT in the image fusion field, there are several aspects that have yet to be resolved. One aspect is the precise selection of the information extracted from each of the source images; and the control of the trade-off between the spatial and spectral quality of the fused image. Indeed, it can be affirmed that multiresolution transforms with low anisotropy are not capable of intrinsically controlling this trade-off. On the other hand, it should be noted that the multidimensional versions of these transforms are built from 1-D bases. Thus the 2-D version, for example, is capable to detect discontinuities from single points, but does not favour their integration into continuous segments. Consequently these 2-D transforms cannot detect efficiently smooth discontinuities Do & Vetterli (2001). That is one of the reasons that justifies the search of new image representations, defined by bases that match image dimensionality. The appearance of new transforms, such as Curvelets Candès & Donoho (1999a), Ridgelets Candès & Donoho (1999b) and Contourlets Do & Vetterli (2005), which improves the 2-D information representation with respect to the DWT, opens a new field of research in the image fusion algorithms area. Generally speaking, it can be affirmed that these new transforms (multiresolution-multidirectional) are based on the application of a double filter bank; the first one is for stepping from a higher to a lower resolution level. The second is a directional filter bank and it allows capturing the directional features for each one of the different resolution levels. They are highly anisotropic and produce a much more efficient extraction of spatial details in different directions, which makes them especially adequate to perform the fusion process. Different published works address this issue. Choi et al. (2005) proposed the use of the Curvelet Transform, while Qiguang & Baoshu (2006) used a Contourlet transform, to fuse satellite images recorded by a panchromatic sensor and a multispectral sensor.

In order to reduce the cost involved in a double filter bank, in Lillo-Saavedra & Gonzalo (2007) a fusion method was proposed based on a new joint MultiDirectional and MultiResolution (MDMR) image representation that uses a single Directional Low Pass Filter Bank (DLPFB) defined in the frequency domain. As shown in the present paper, this new methodology has the intrinsic capacity to control the global quality (spatial-spectral) of the fused images. This control is based on the accurate tune-up of the DLPFB. The aim of this paper is to propose a method that objectively determines the design of the DLPFB. Specifically, it proposes the optimization of an objective function (OF) based on fused image quality measures, using the Simulated Annealing (SA) search algorithm.

2. Background

2.1 A MDMR representation for image analysis and synthesis

Lillo-Saavedra & Gonzalo (2007) proposed a joint MDMR representation that combines the simplicity of the Wavelet Transform, calculated using the *à trous* algorithm (WAT), with the benefits of multidirectional transforms like Contourlet Transform (CT), using a single DLPFB. Thus, at each decomposition level (θ_n), image degradation is performed applying a directional low pass filter in the frequency domain, as shown in Equation 1.

$$\text{Image}_{\theta_n}(x,y) = FFT^{-1}\left\{FFT\left\{\text{Image}_{\theta_{n-1}}(x,y)\right\} \cdot H_{\theta_n}(u,v)\right\} \tag{1}$$

Where θ_n is the decomposition level prior to transform application and represents the directional low pass filter transfer function, applied in level n. The directional information is extracted by the difference of the directional degraded images in two consecutive levels and is stored in the transforms coefficients at each level:

$$Coef_{\theta_n}(x,y) = \text{Image}_{\theta_n}(x,y) - \text{Image}_{\theta_{n-1}}(x,y) \qquad (2)$$

From Equations (1) and (2), the original image can be exactly reconstructed by Equation (3):

$$\text{Image}(x,y) = \text{Image}_{\theta_k}(x,y) + \sum_{n=1}^{k} Coef_{\theta_n}(x,y) \qquad (3)$$

In other words, it adds to the corresponding image at the higher decomposition level (θ_k) all the directional coefficients, ($Coef_{\theta_n}$), in a procedure analogous to the one used in WAT.

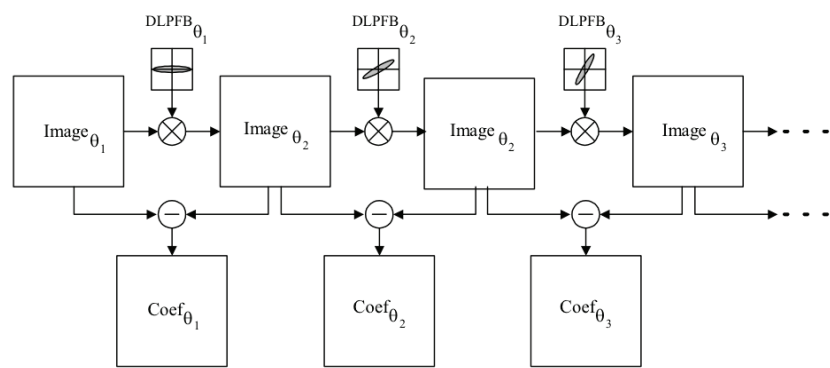Fig.1 illustrates graphically the joint MDMR representation.

Fig. 1. Flow diagram of a MDMR image representation based on a directional low pass filter bank.

For computational reasons it is highly desirable that the directional low pass filter transfer function $H_{\theta_n}(u,v)$ could be defined as a separable function. However, Lakshmanan (2004) demonstrated that a low pass filter that is simultaneously separable and directional could not exist. But, it is possible to define a directional low pass filter as the sum of two separable filters as shown in Equation (4):

$$H_{\theta_n}(u,v) = H_1(u) \times H_2(v) - \alpha u H_1(u) \times v H_2(v) \qquad (4)$$

Where α is given by the relation $(a^2 - b^2)\sin(2\theta)/(a^2b^2)$, being θ, a and b the orientation, scale and elongation of the filter, respectively and H_1 and H_2 are defined as:

$$H_1(u) = \exp(-u^2(\frac{\cos^2\theta}{a^2} + \frac{\sin^2\theta}{b^2})) \qquad (5)$$

$$H_2(v) = \exp(-v^2(\frac{\cos^2\theta}{b^2} + \frac{\sin^2\theta}{a^2})) \qquad (6)$$

The most interesting characteristic of this kind of filters is not its elliptic form, but rather its directional character by which it assigns higher weights to the corresponding values in a determined direction and lower weights to its orthogonal direction. From a practical point of view, it should be also noted that the filtering results depend also strongly on the number of partitions of the frequency space (k) and the number of elements that define the filter size (m). On the other hand, given the symmetrical nature of Fourier space where the DLPFB is applied, filters must be also symmetrical.

2.2 Fusion methodology based on a MDMR representation

Similar to other fusion methods for multispectral (MULTI) and panchromatic (PAN) images, the objective of the fusion methodology investigated in this work is to coherently integrate the low frequency information from the MULTI image and the high frequency information from the PAN image, to obtain a fused image whose spatial quality would be as similar as possible to the quality of the higher resolution spatial image (PAN), while conserving the spectral characteristics of the high resolution spectral image (MULTI).

Under the previous considerations, Lillo-Saavedra & Gonzalo (2007) formalized a new images fusion methodology based on the MDMR representation described previously:

$$FUS^i(x,y) = MULTI^i_{\theta_k}(x,y) + \sum_{n=1}^{k} Coef^{PAN}_{\theta_n}(x,y) \tag{7}$$

Where $FUS^i(x,y)$ represents the i-th spectral band of the fused image, $MULTI^i_{\theta_k}(x,y)$ represents the ith band of the MULTI image degraded in k directions, and $Coef^{PAN}_{\theta_n}(x,y)$ represents the PAN image coefficients (Equation (2) and Fig.1).

The described methodology presents two relevant features: its high anisotropy and the control of the inherent compromise between spatial and spectral quality of the fused image; in particular, and as it will be showed, it is possible to obtain fused image with an equalized trade-off between both qualities. In this sense, it is important to note that the values of the filter parameters (*a* and *b*) determine the geometry of the low pass filters that conform DLPFB and therefore the information of the image that will retain the coefficients, and each of the degraded images, which is determinant of the final quality of the fused image. A sensitivity analysis of the spatial and spectral quality of the fused images against these parameters has been performed in Gonzalo & Lillo-Saavedra (2008). From this study, it was concluded that the potential of the proposed fusion methodology would be strengthened if a filter parameters tune-up method would be available.

2.3 Quality measure of fused images

In the literature, it can be found some quality indices, which measure fused images quality from different perspectives Vijayaraj et al. (2006); Wang & Bovik (2002); Zhou et al. (1998). In this chapter, the fused images quality have been measured using spectral ERGAS (Erreur Relative Globale Adimensionnelle de Synthèse, Wald (2002) and spatial ERGAS Lillo-Saavedra et al. (2005) quality indexes. The original definition of the ERGAS index was proposed by Wald (2000) through the Equation (8):

$$ERGAS_{spectral} = 100\frac{h}{l}\sqrt{\frac{1}{N_{Bands}}\sum_{i=1}^{N_{Bands}}\left(\frac{(RMSE_{spectral}(Band^i))^2}{(MULTI^i)^2}\right)} \tag{8}$$

Where h and l represent the spatial resolution of the PAN and MULTI images, respectively; N_{Bands} is the number of bands of the fused image; $MULTI^i$ is the mean radiance value of the ith band of the MULTI image. The $RMSE$ (Root Mean Square Error) is evaluated through Equation (9):

$$RMSE_{spectral}\left(Band^i\right) = \frac{1}{NP}\sqrt{\sum_{j=1}^{NP}\left(MULTI^i(j) - FUS^i(j)\right)^2} \tag{9}$$

being NP the number of pixels of the fused image. It is clear, from its definition, that low ERGAS index values represent high quality of the fused images. Although the original ERGAS index was defined as a global quality index. In Lillo-Saavedra et al. (2005), it is showed that their behaviour is rather that of a spectral quality index. It is in this sense that the Wald-ERGAS index will be called $ERGAS_{spectral}$ in this chapter. A new index was proposed Lillo-Saavedra et al. (2005) with the objective of evaluating the distance between the PAN image and the FUS image (spatial quality). This index has been named spatial ERGAS, since it is based in the same concept that the original ERGAS. In its definition, a spatial $RMSE$ has been included, which is defined as in Equation (10):

$$ RMSE_{spatial}\left(Band^i\right) = \frac{1}{NP}\sqrt{\sum_{j=1}^{NP}\left(PAN^i(j) - FUS^i(j)\right)^2} \qquad (10) $$

Where PAN^i is the image obtained by adjusting the histogram of the original PAN image to the histogram of the ith band of the FUS image. In this way the spectral differences between the PAN and FUS images are minimized. Therefore, replacing $RMSE_{spectral}$ by $RMSE_{spatial}$ and $MULTI^i$ by PAN^i in the Equation (8), next expression is obtained:

$$ ERGAS_{spatial} = 100\frac{h}{l}\sqrt{\frac{1}{N_{Bands}}\sum_{i=1}^{N_{Bands}}\left(\frac{(RMSE_{spatial}(Band^i))^2}{(PAN^i)^2}\right)} \qquad (11) $$

This index is able to quantify the spatial quality of fused images by measuring the PAN and FUS image distance, in the same sense of Wald-ERGAS index, discussed above, does for spectral quality.

3. Materials and methods

3.1 Data description

In this study, two scenes registered by the panchromatic and multispectral sensors on board IKONOS and QUICKBIRD satellites, respectively, have been used. Table 1 summarizes spectral and spatial characteristics of these sensors. For both two scenes, the multispectral image size was 128x128 pixels and consequently the size of PAN images are 512x512. The IKONOS scene was recorded on March 10, 2000, and it is geographically located in the Maipo Valley, near Santiago, Chile. The QUICKBIRD scene was extracted from an image recorded on August 22, 2002, and geographically corresponds to the northwest area outside of Madrid, Spain. PAN images of these scenes are presented in Fig. 2 (a) and (d), and NGB (NearIR-Green-Blue) compositions of their corresponding MULTI images in 2 (b) and (e).

	QUICKBIRD		IKONOS	
Band	Spatial Res. (m)	Spectral Res. (μm)	Spatial Res.	Spectral Res. (μm)
B1		0.450-0.520		0.445-0.516
B2	2.44	0.520-0.600	4 m	0.506-0.595
B3		0.630-0.690		0.632-0.698
B4		0.760-0.900		0.757-0.853
PAN	0.61	0.450-0.900	1 m	0.450-0.900

Table 1. Characteristics of the multispectral and panchromatic sensors on board IKONOS and QUICKBIRD platforms
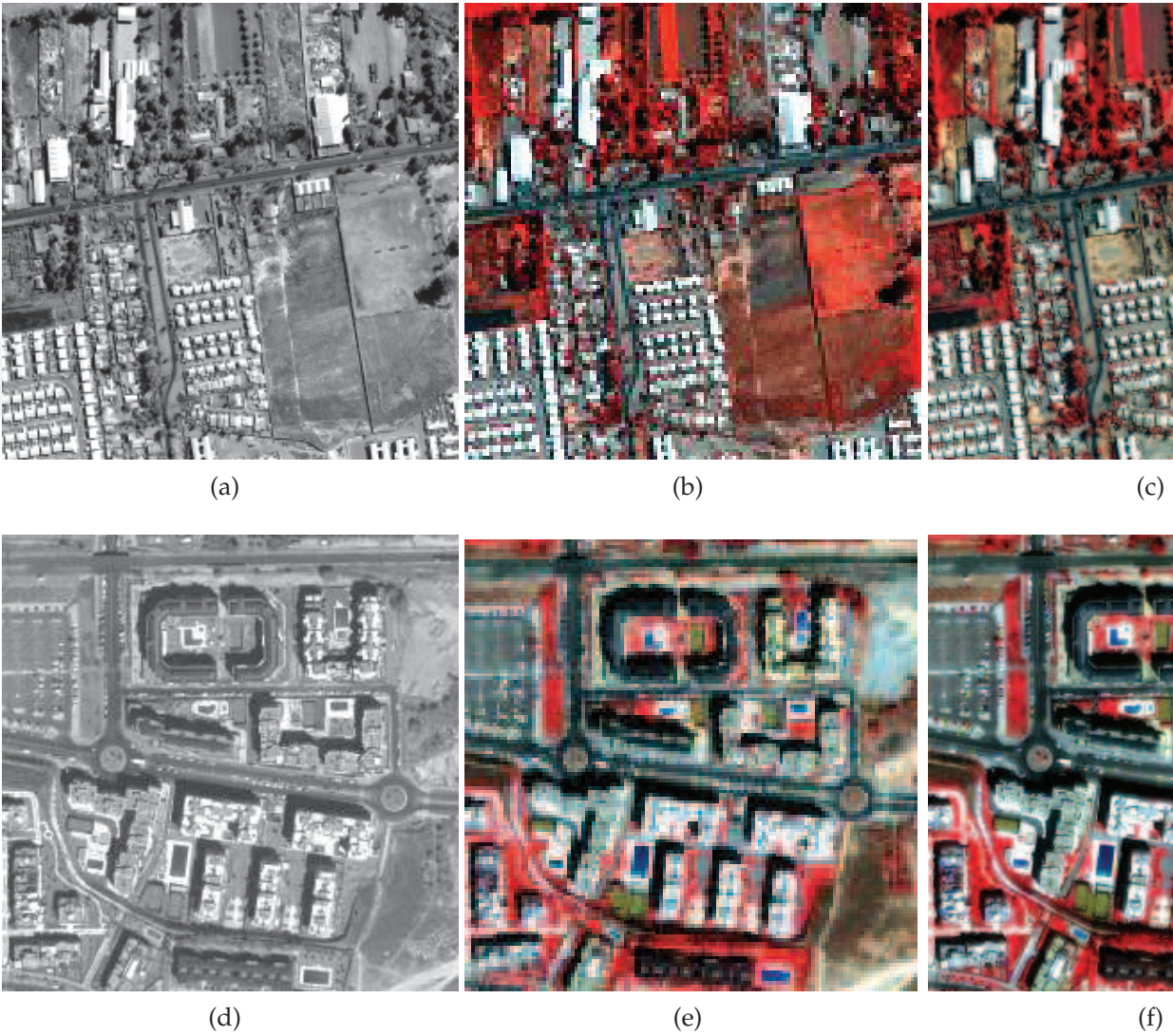
Fig. 2. Source images. First row: IKONOS scene. (a) PAN image. (b) NGB composition of MULTI image. (c) FUS image. Second row: QUICKBIRD scene. (d) PAN image. (e) NGB composition of MULTI image. (f) N image.

3.2 Search algorithm description

The search algorithm proposed in this paper is based on the SA optimization method developed by Kirkpatrick et al. (1983) and it pertains to a wide class of local search algorithms, known as Threshold Algorithms Ingber (1993). The principles of the SA optimization method is based on the physical analogy with the behavior of a set of atom nuclei, approximating to the thermodynamic equilibrium at a determined temperature, understanding a thermodynamic equilibrium as that state in which there is no energetic exchange between system components. Every time that the process iterates, the SA searches a new solution that lies in the vicinity of the actual one. Then, the difference between an objective function (OF) associated with each solution is calculated. If the difference is less than a certain threshold, then the new solution becomes the actual one and the process is repeated. In the SA algorithm is necessary a random variable that follows a certain probability function with values between 0 and infinity. The acceptance of worse solutions is governed by the following criterion:

$$rand(0,1) < e^{(OF(x_{i+1})-OF(x_i))/T} \qquad (12)$$

Where T represents a parameter that receives the name of temperature and $rand(0,1)$ is a random number between 0 and 1 with an uniform probability distribution. The SA strategy begins with an initially high temperature, which provides a high probability to accept movements that worsen OF. In each iteration, the temperature is reduced, diminishing the probability of accepting worse solutions. This temperature reduction process is known as the cooling schedule and is controlled by the temperature decrease index (δ). A very small δ value implies a rapid convergence; however, this means that the search is not exhaustive, increasing the probability of getting confined at a local minimum. In contrast, with a high δ value, the search algorithm converges more slowly since it is more exploratory, increasing the probability of obtaining solutions close to the global minimum.

3.3 Definition of the OF

Even though other OFs can be defined, depending on the final fused image application, in this chapter, this function has been defined with the objective of obtaining a fused image with the spatial and spectral quality balanced. Thus the OF has been defined by the difference between spatial and spectral ERGAS indices, as formalized in Equation (13):

$$\Delta E = \left| ERGAS_{spatial} - ERGAS_{spectral} \right| \qquad (13)$$

3.4 Methodology for searching filter parameters

Before carrying out a blind search for the parameters a and b using the SA algorithm, it has been considered highly recommended the study of the influence of these parameters on the indices ERGAS. For that, a high number of fused images have been generating by varying a and b from 0 to 5 and different values of k. The obtained surfaces for spatial ERGAS, spectral ERGAS and their average are represented at Fig. 3, for $k = 2^3$.

In Fig.3, it can observe that an increase in parameter values diminishes the spectral quality of fused images while increases their spatial quality and vice versa. Therefore, there is a set of a and b values that establishes a balance between spatial and spectral quality of fused images. On the other hand, it can be noted in Fig. 3 that the parameters a and b present a symmetrical behaviour with respect to the principal diagonal of the space defined by them. This symmetry has been checked for a large number of cases. As a result, this condition has been also imposed in the search space. Derived from this fact, an oriented search criterion has been established:
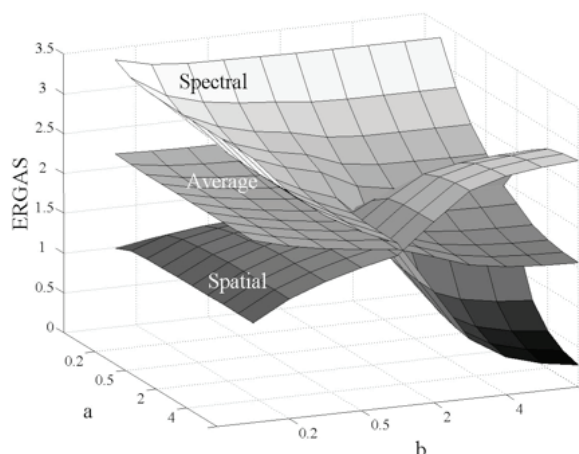
Fig. 3. Surfaces of spatial and spectral ERGAS and their average values for a fused image with $k = 2^3$

if the OF value is less than zero ($ERGAS_{spatial} < ERGAS_{spectral}$), then the spectral quality should be improved in diminishment of the spatial quality of the fused image and vice versa in the opposite case, for OF greater than zero, the spatial quality of the fused image should be increased. Introducing these considerations in the classical SA algorithm, the methodology applied for searching filter parameters can be illustrated by the flow diagram represented at Fig. 4.

As it can be saw at Fig. 4, the input to the algorithm are the two pre-processed source images: the PAN and one spectral band of the MULTI image. Then filter parameters are initialized (k, m, a_{ini} and b_{ini}) for generating an initial filter. With this first filter, a fused image (Equation 7) is obtained and an initial value of OF (Equation 13) is calculated. Next, filter parameters, a and b, should be updated according to the oriented search criterion established above. For that a and b parameters should be modified in the right direction. In this sense, the terms da and db are defined for increasing or decreasing current values of a and b as:

$$da = |\Delta E_{ini}| \, rand \qquad (14)$$

$$db = |\Delta E_{ini}| \, rand \qquad (15)$$

As it can observe in Equations 14 and 15, da and db take random values scaled in the ΔE_{ini} range, which decreases with the algorithm convergence.

Once the new solution ΔE_{end} is obtained from the new parameters ($a_{end} = a_{ini} \pm da$ and $b_{end} = b_{ini} \pm db$), it is compared with ΔE_{ini}, then if it is lower the new solution is accepted, in otherwise it will be accepted or discarded according to the SA acceptance criterion (Equation 12). Thus in each iteration a new fused image is obtained and a new OF solution is calculated and compared with the previous one to go to next SA iteration, after decreasing the T value through the δ parameter ($\delta < 0$).

4. Results

The methodology described above allows to determine in an objective way the a and b parameters; however, the quality of images fused using the described fusion methodology is determined also by other DLPFB parameters: filter size (m) and the number of partitions of the frequency space (k). It is noteworthy to do some considerations about these two parameters.
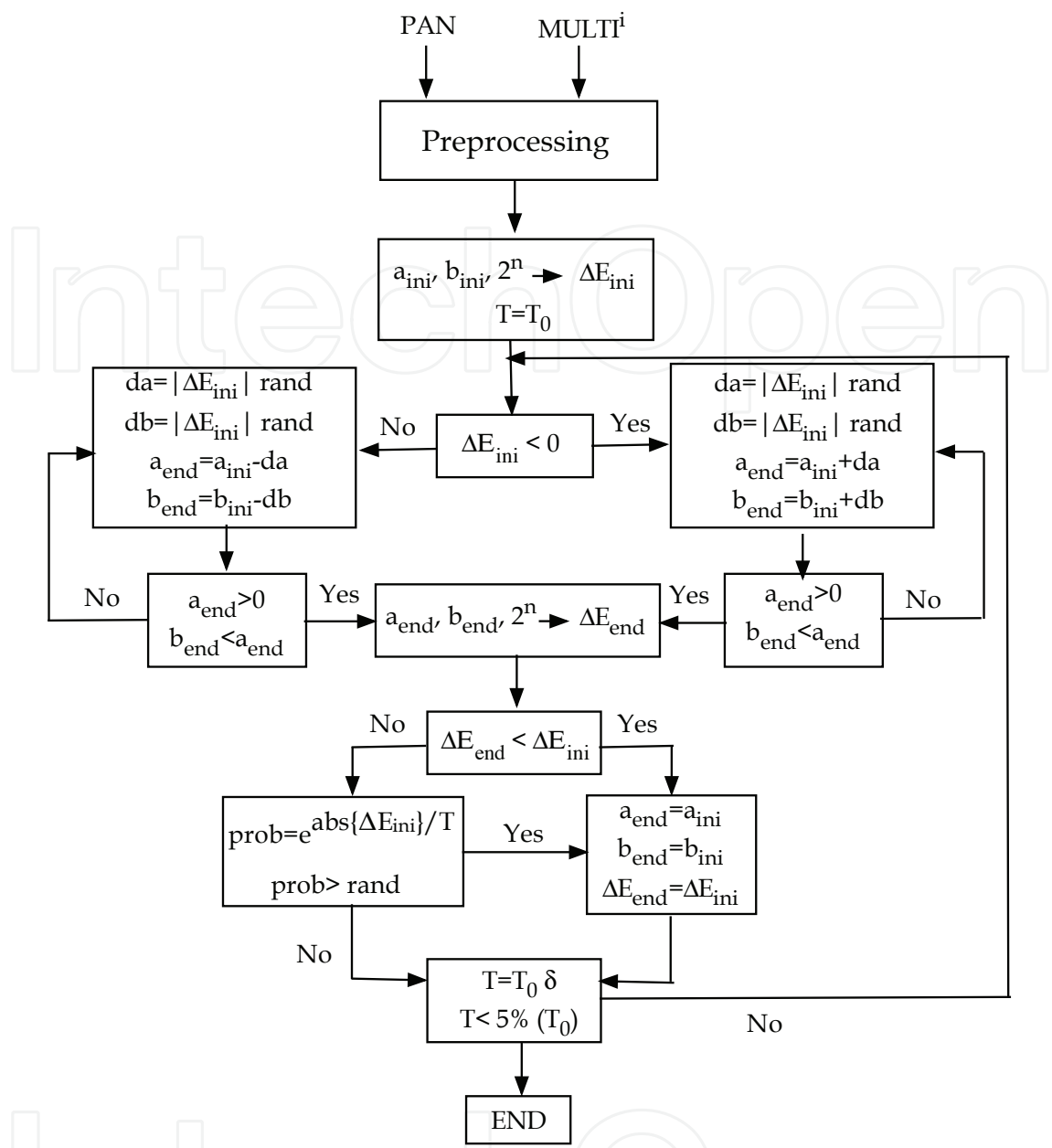
Fig. 4. Flow chart of the directed search algorithm

Experimentally, it was observed that $m = 5$ is the minimal number of samples required to define a symmetric kernel of this type of filters (Equation 4). Other kernel sizes that maintain the symmetry are $m = 11$ and $m = 21$, which present similar behaviour. However, an increase in size implies an elevated increase in computational complexity. On the other hand, empirical studies have shown that for frequency space partitions (k) varying between 2^2 and 2^6, there is a pair of values (a, b) that provides very similar spatial and spectral qualities.

Before applying the SA searching algorithm for obtaining a pair of parameter values (a and b) which provides a fused image with spatial and spectral quality balanced, for each scene, the dependence of OF on filter parameters have been investigated. For that, the two selected scenes (IKONOS and QUICKBIRD) have been fused by varying a and b (from 0 to 10), m (equal to 5, 11 and 21) and k (equal to 2^3 and 2^4). After that, objective functions have been evaluated for each set of values. Fig (5) presents a summary of OF's surfaces: the first row of

Fig. (5) corresponds to the IKONOS scene and the second row to the QUICKBIRD scene. The surfaces presented in the 1st and 2nd column correspond to the images fused with a 5-sample filter bank and a frequency space partition of 2^3 and 2^4, respectively; while the 3rd and 4th columns correspond to a 21-sample filter size with the same partitions for the frequency space. One of the most notable aspects in the surfaces shown in Fig. (5) is the presence of valleys. That means, for all analyzed cases, there is a set of pairs of parameter values, a and b, for which the objective function takes minimum values. That justifies the use of a search method based on certain rules to find the parameters that optimize the OF in few iterations.

With the goal of determining the value of the temperature decreasing factor, δ, that provides the best compromise between algorithm convergence velocity and search efficiency, in terms of fused images quality, different pairs of parameters a and b have determined through the search algorithm for δ values equal to 0.4, 0.6 and 0.8. Results indicated that δ values greater or equal to 0.8 provide the best results, since a high δ values reduce the convergence velocity, this last value has used in all experiments carried out in this study.

Different experiments have been performed, in order to analyze the convergence behaviour of the search algorithm. General speaking, it can affirm that the quality of the results obtained using the SA algorithm is independent of initial values of parameters Kirkpatrick et al. (1983). In Fig. 6, it can appreciate that for different initial MDMR filter parameter values (a_{ini} and b_{ini}), the final (ΔE) value is the same.

In order to assess the influence of the oriented search criterion proposed in this work, on the SA algorithm convergence, average values for the number of iterations required for converging have been estimated, without the search criterion and with it. Fig. 7 shows these results for the IKONOS scene. Fig. 7 (a) and 7 (b) show the evolution of ΔE, da and db without the directed search criterio and Fig. 7 (c) and 7 (d) with it. It can appreciate as the convergence is much faster when the oriented criterion is applied. It should be noted that this is a critical aspect in applications where the OF estimation implies a high computational complexity, like it is the images fusion problem.

Applying the oriented SA algorithm, for $k = 2^3$, $m = 5$ and $\delta = 0.8$, values of a and b were obtained for each scene and for each spectral band. The obtained values have summarized at Table 2. IKONOS and QUICKBIRD scenes have been fused with the parameter values included in Table 2 through the MDMR method. NGB compositions of fused images are presented in Fig.2 (c) and 2 (f), respectively. It should be noted that a visual comparison with the multispectral images (2 (b) and 2 (e)), shows a noteworthy improvement in spatial quality while maintaining spectral quality.

SCENE	B1		B2		B3		B4	
	a	b	a	b	a	b	a	b
IKONOS	0.7035	1.4081	0.8848	1.9519	0.8833	1.9199	0.8380	1.8354
QUICKBIRD	0.5670	1.7205	0.7973	1.8117	0.8240	2.0493	0.7014	1.5462

Table 2. Filter parameters determined using the oriented search algorithm

The two scenes were fused as well, using other fusion methods based on different transformations: IHS Tu et al. (2004), Wavelet-Mallat (WMT) Mallat (1989) and Wavelet-*á trous* (WAT) Nunez et al. (1999). Fig.8 presents details of two particular areas, one per scene, of original MULTI images (a) and (f), and the corresponding images fused by the four fusion methods: IHS ((b) and (g)), WMT ((c) and (h)), WAT ((d) and (i)) and MDMR((e) and (j)). A comparative visual analysis between these details indicates that the fusion methods WMT and MDMR conserve more faithfully the original images spectral content for the two scenes.
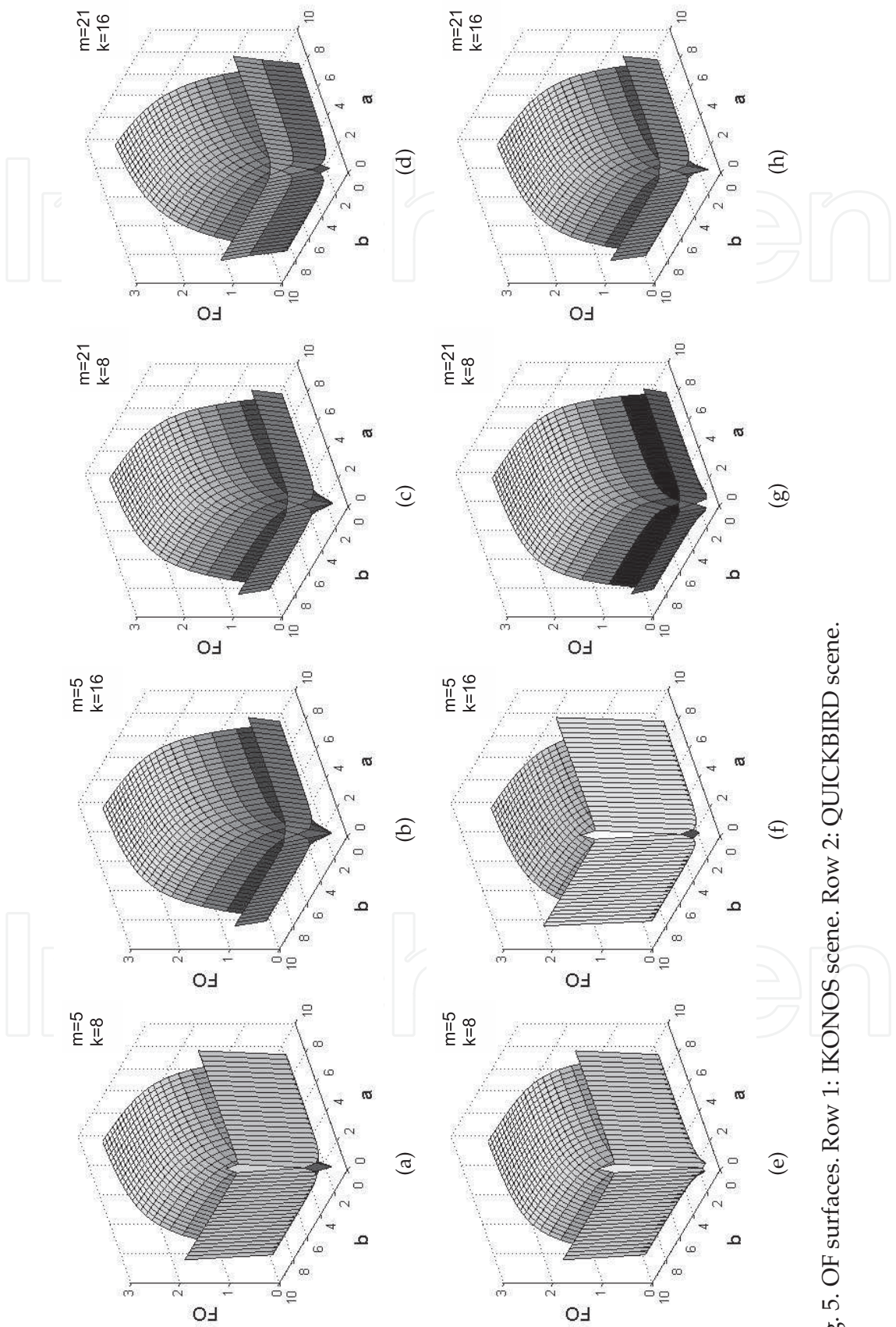
Fig. 5. OF surfaces. Row 1: IKONOS scene. Row 2: QUICKBIRD scene.
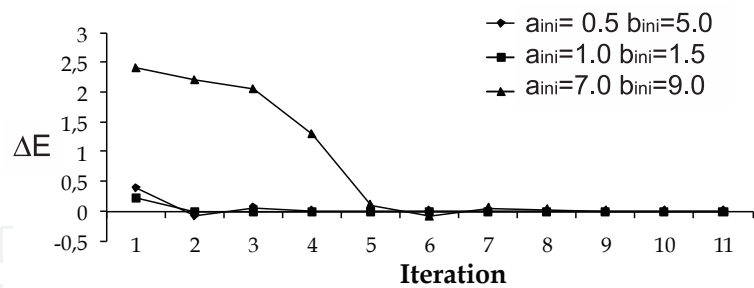
Fig. 6. Convergence of the SA search algorithm for different initial conditions of the filter bank parameters
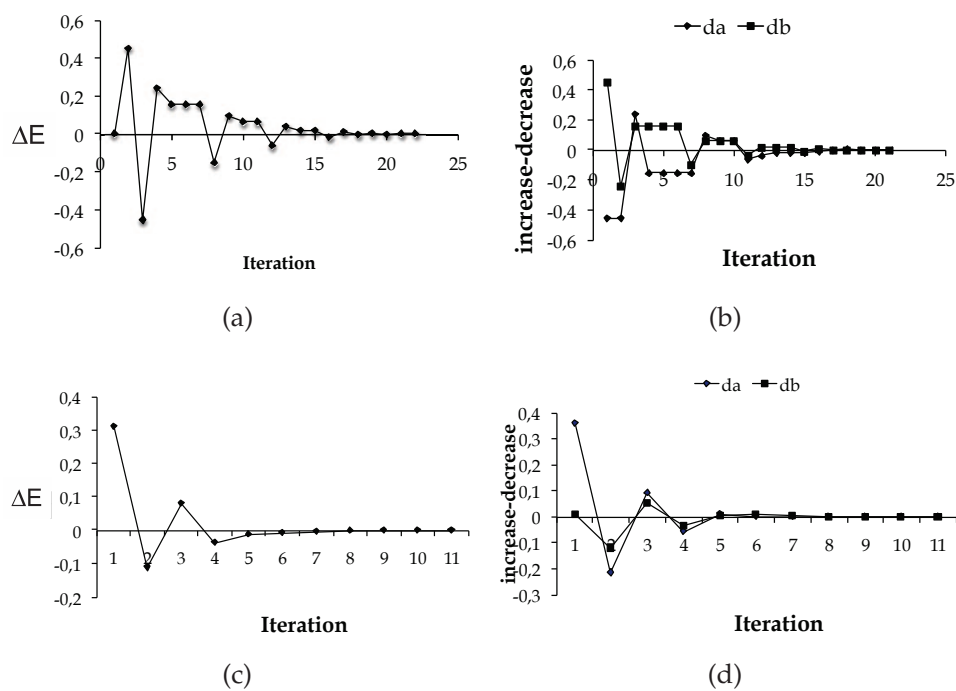

(a)

(b)

(c)

(d)

Fig. 7. Evolution of ΔE, *da* and *db* without the directed search criterio (a) and (b) and with it (c) and (d)

Moreover, the presence of artefacts that worsen spatial quality can be appreciated in Fig.8 (b), (c), (g) and (h) while they are absent in Fig.8 (d), (e), (i) and (j).

In order to quantify the results previously exposed, ERGAS (spatial and spectral) index values as well as its average and standard deviation were calculated. The two last indices represent a global quality measure and a measure of the trade-off between spatial and spectral quality, respectively. Values of indices are included in Table 3 for IKONOS scene and in 4 for QUICKBIRD scene. In these tables, it can observe that the lowest $ERGAS_{spatial}$ value, and therefore the best spatial quality, is given by the WAT method, although it does not result in a balance between spatial and spectral quality, as the value of standard deviation reflects. However, the MDMR method gives a total equilibrium between spatial and spectral quality. And additionally, this method provides fused images with the best spectral quality, since the corresponding $ERGAS_{spectral}$ values are lower than for the other methodologies.
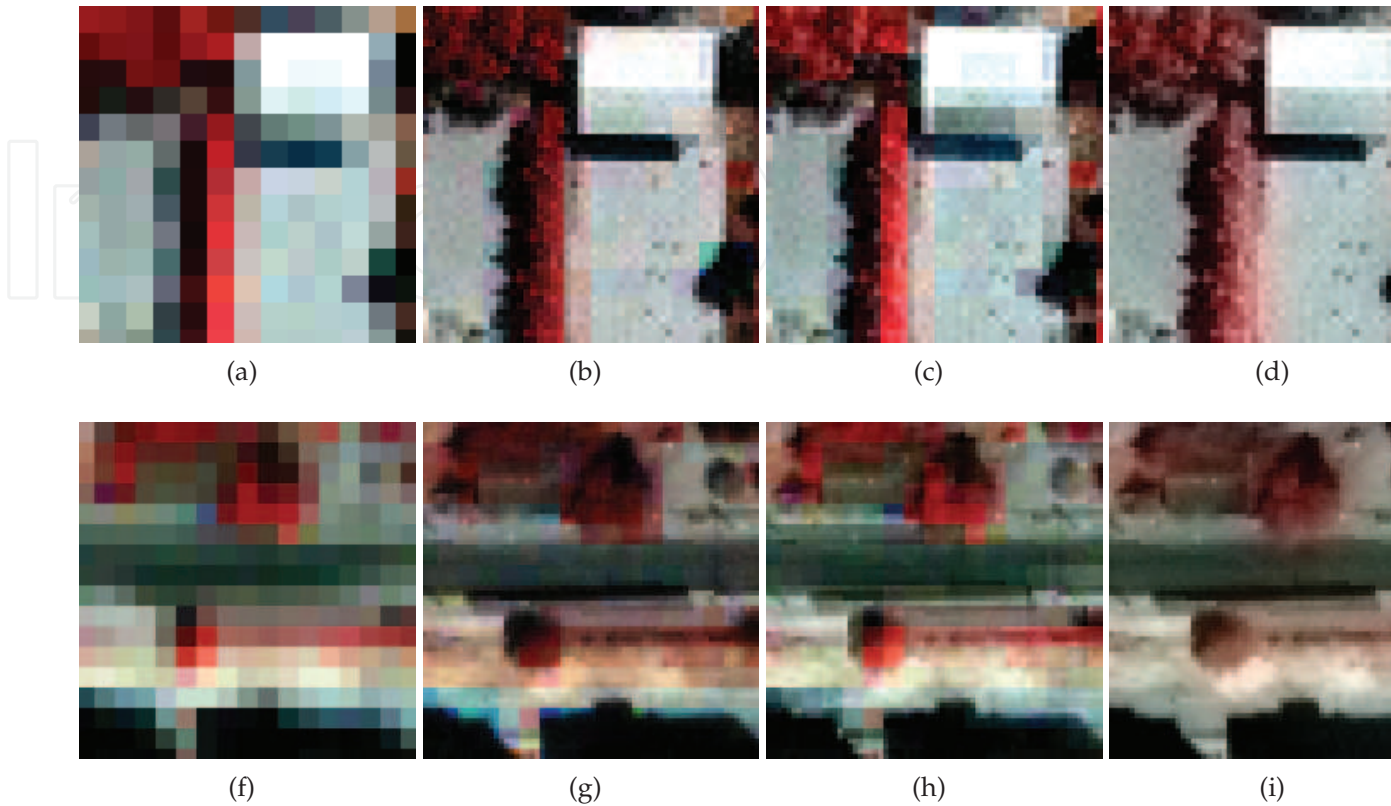
(a) (b) (c) (d)

(f) (g) (h) (i)

Fig. 8. Details of original MULTI images and fused images. First row: IKONOS scene. Second row: Q
MULTI images: (a) and (f) . Fused images: IHS method ((b) and (g)), WMT method ((c) and (h)), WAT
MDMR method ((e) and (j)).

FUSION METHOD	$ERGAS_{spatial}$	$ERGAS_{spectral}$	Average	St. Dev.
IHS	1.9931	2.6574	2.3252	0.6643
WMT	2.0790	2.2083	2.1436	0.1293
WAT	**1.7067**	2.3029	2.0048	0.5692
MDMR	1.9226	**1.9226**	1.9226	0.0000

Table 3. ERGAS Values for the fused IKONOS scene

FUSION METHOD	$ERGAS_{spatial}$	$ERGAS_{spectrall}$	Average	St. Dev.
IHS	1.8860	2.5938	2.2399	0.5004
WMT	2.1334	1.7731	1.9533	0.2548
WAT	**1.7079**	1.8822	1.7951	0.1233
MDMR	1.7627	**1.7627**	1.7627	0.0000

Table 4. ERGAS values for the fused QUICKBIRD scene

5. Conclusions

In this chapter, it has been proposed a search algorithm, based on the Simulating Annealing, which improves the global quality of satellite images fused through a fusion algorithm based on a joint MDMR representation.

In a first phase, the search algorithm has been implemented for carrying out an exhaustive exploration of the space defined by two parameters (elongation and scale), involved in design of the filter bank used by the fusion algorithm. The analysis of the influence of these parameters on the fused images quality has allowed establishing an oriented search criterion, which reduces significantly the number of iterations requiered for converging. This search algorithm can be applied to different functions. But, since the aim of this work is to get fused images with the spatial and spectral quality balanced, here OF has been defined as the difference of two quality indices: one spatial and one spectral.

Experimental results have proved that the convergence of the algorithm is independent on initial conditions and that the number of iterations is significatively reduced when the oriented criterion is applied.

From the qualitative and quantitative analysis of the fused images quality, it can be concluded that the MDMR fusion methodology complemented with the oriented search algorithm, which is proposed in this paper, provides fused images with a higher spectral quality than the other algorithms evaluated; and spatial quality comparable to that offered by the WAT method. Still, the most notable feature of the proposed methodology is that it provides a total balance between the two qualities, spatial and spectral, for the two kind of images used.

6. References

Candès, E. J. & Donoho, D. L. (1999a). *Curve and Surfaces*, Vanderbilt University Press., chapter Curvelets - A Surprisingly Effective Nonadaptive Representation For Objects with Edges.
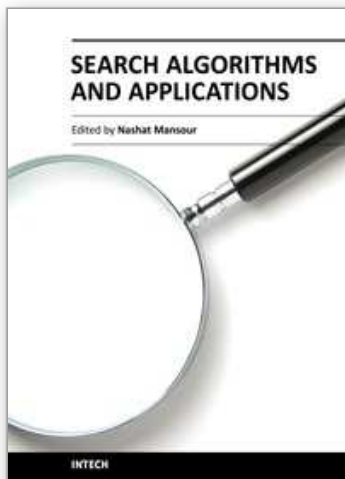
Candès, E. J. & Donoho, D. L. (1999b). Ridgelets: A key to higher-dimensional intermittency?, *Philosophical Transactions of the Royal Society* 357: 2459–2509.

Candès, E. J. & Donoho, D. L. (2000). Curvelets, multiresolution representation, and scaling laws, *in* A. Aldroubi, A. Laine & M. Unser (eds), *Wavelet Applications in Signal and Image Processing VIII*, number 4119, SPIE, pp. 1–12.

Chibani, Y. & Houacine, A. (2003). Redundant versus orthogonal wavelet descomposition for multisensor image fusion, *Pattern Recognition* 36(4): 879–887.

Choi, M., Young, K. R., Nam, M. R. & Kim, H. O. (2005). Fusion of multispectral and panchromatic satellite, images using the curvelet transform, *IEEE Transactions on Geoscience and Remote Sensing Letters* 2(2): 136–140.

Do, M. N. & Vetterli, M. (2001). Pyramidal directional filter banks and curvelets, *In International Conference in Image Processing*, Vol. 3, pp. 158–161.

Do, M. N. & Vetterli, M. (2005). The contourlet transform: an efficient directional multiresolution image representation, *IEEE Transactions on Image Processing* 14(12): 2091 – 2106.

Dutilleux, P. (1989). An implementation of the algorithm à trous to compute the wavelet transform, *in* J. Combes, A. Grossmann & P. Tchanitchian (eds), *Compt-rendus du congrès ondelettes et mèthodes temps-frèquence et espace des phases*, Springer-Verlag, pp. 298–304.

Garguet-Duport, B., Girel, J., Chassery, J. & Pautou, G. (1996). The use of multiresolution analysis and wavelets transform for merging spot panchromatic and multispectral image data, *Photogrammetric Engineering and Remote Sensing* 62(9): 1057–1066.

Gonzalo, C. & Lillo-Saavedra, M. (2008). A directed search algorithm for setting the spectral-spatial quality trade-off of fused images by the wavelet à trous method, *Canadian Journal of Remote Sensing* 34(4): 367–375.

Ingber, L. (1993). Simulated annealing: practice versus theory, *Math. Comput. Modelling* 18(11): 29–57.

Kirkpatrick, S., Gelatt, C. D. & Vecchi, M. P. (1983). Optimization by simulated annealing, *Science* 4598(220): 671–680.

Lakshmanan, V. (2004). A separable filter for directional smoothing, *IEEE Transactions on Geoscience and Remote Sensing Letters* 1(3): 192–195.

Lillo-Saavedra, M. & Gonzalo, C. (2007). Multispectral images fusion by a joint multidirectional and multiresolution representation, *International Journal of Remote Sensing* 28(18): 4065–4079.

Lillo-Saavedra, M., Gonzalo, C., Arquero, A. & Martinez, E. (2005). Fusion of multispectral and panchromatic satellite sensor imagery based on tailored filtering in the fourier domain, *International Journal of Remote Sensing* 26(6): 1263–1268.

Malfait, M. & Roose, D. (1997). Wavelet-based image denoising using a markov random field a priori model, *IEEE Transactions on Image Processing* 6(4): 549–656.

Mallat, S. G. (1989). A theory for multiresolution signal decomposition: The wavelet representation, *IEEE Transactions on Pattern Analysis and Machine Intelligence* 2(7): 674–693.

Nunez, J., Otazu, X., Fors, O., Prades, A., Pala, V. & Arbiol, R. (1999). Multiresolution-based image fusion with additive wavelet decomposition, *IEEE Transactions on Geoscience and Remote Sensing* 37(3): 1024–1211.

Pohl, C. & J.L.Genderen (1998). Multisensor image fusion in remote sensing: Concepts, methods and application, *International Journal of Remote Sensing* 19(5): 823–854.

Qiguang, M. & Baoshu, W. (2006). The contourlet transform for image fusion, *in* B. V. Dasarathy (ed.), *Information Fusion: Architectures, Algorithms and Applications*, Vol. 6242, SPIE.

Ranchin, T. & Wald, L. (2000). Fusion of high spatial and spectral resolution image: The arsis concept and its implementation, *Photogrammetric Engineering and Remote Sensing* 66(1): 49–61.

Tu, T., Huang, P. S., Hung, C. & Chang, C. (2004). A fast intensity-hue-saturation fusion technique with spectral adjustment for IKONOS imagery, *IEEE Transactions on Geoscience and Remote Sensing Letter* 1(4): 309–312.

Unser, M. (1995). Texture classification and segmentation using wavelet frames, *IEEE Transactions on Image Processing* 4(11): 1549–1560.

Vijayaraj, V., O'Hara, C. G. & Younan, N. H. (2006). Quality analysis of pansharpened images, *Optical Engineering* 45(4): 88.

Wald, L. (2002). *Data Fusion: Definitions and Architectures : Fusion of Images of Different Spatial Resolutions*, Les Presses - Mines Paris.

Wang, Z. & Bovik, A. C. (2002). A universal image quality index, *IEEE Signal Processing Letters* 9(3): 81–84.

Yang, S., Wang, M., Jiao, L., Wu, R. & Wang, Z. (2010). Image fusion based on a new contourlet packet, *Information Fusion* 11(2): 78–84.

Zhou, J., Civco, D. L. & Silander, J. A. (1998). A wavelet transform method to merge landsat tm and spot panchromatic data, *International Journal of Remote Sensing* 19(4): 743–757.

Zou, H. & Jiang, J. (2010). A texture image recognition method based on the contourlet transform and biomimetic pattern recognition, *Computer Engineering and Science* 01.

Search Algorithms and Applications

Edited by Prof. Nashat Mansour

Search algorithms aim to find solutions or objects with specified properties and constraints in a large solution search space or among a collection of objects. A solution can be a set of value assignments to variables that will satisfy the constraints or a sub-structure of a given discrete structure. In addition, there are search algorithms, mostly probabilistic, that are designed for the prospective quantum computer. This book demonstrates the wide applicability of search algorithms for the purpose of developing useful and practical solutions to problems that arise in a variety of problem domains. Although it is targeted to a wide group of readers: researchers, graduate students, and practitioners, it does not offer an exhaustive coverage of search algorithms and applications. The chapters are organized into three parts: Population-based and quantum search algorithms, Search algorithms for image and video processing, and Search algorithms for engineering applications.

How to reference

In order to correctly reference this scholarly work, feel free to copy and paste the following:

Consuelo Gonzalo-Martín and Mario Lillo-Saavedra (2011). Balancing the Spatial and Spectral Quality of Satellite Fused Images through a Search Algorithm, Search Algorithms and Applications, Prof. Nashat Mansour (Ed.), ISBN: 978-953-307-156-5, InTech, Available from: http://www.intechopen.com/books/search-algorithms-and-applications/balancing-the-spatial-and-spectral-quality-of-satellite-fused-images-through-a-search-algorithm

INTECH

open science | open minds